# THE SOLUTION TO FIXED END FORCE OF PRISMATIC MEMBERS WITH BIMODULUS AND EQUAL SECTION

Yangjun MENG[1,*], Can LI[2]

*This research advances the engineering application of bimodular materials by developing a program for calculating the geometric characteristics of any cross-section, utilizing bimodular theory and a binary iterative method. Additionally, a method for computing fixed-end forces in prismatic, uniform cross-section bimodular members (for propped cantilever and fixed-end beams) is established using the force method. The calculations for various loads are performed and verified against ANSYS solid element simulations. Analysis of geometric characteristics across various sections reveals that flexural rigidity differs between positive and negative moment regions in generally asymmetric sections, with the exception of symmetric shapes such as rectangles. ANSYS software analysis verification shows that: The derived formulas for fixed end force are accurate and effective, and there is a certain range of reversal of bending moment, the zero moment section spans a certain region, it is not an abrupt point. For a rectangular beam, bimodular analysis reveals an internal force distribution identical to the single-modulus case but a vastly different deflection, as the elastic stiffness no longer equals the flexural rigidity. For asymmetric bimodular sections under load, the internal force distribution diverges from the single-modulus model, yielding significant deflection errors. A high tensile-to-compressive modulus ratio beyond a specific threshold leads to unacceptable errors: over 5% in fixed-end force and over 30% in deflection. So, Frame analysis of internal forces and displacements must consider the bimodulus characteristics of the material.*

**Keywords:** Bimodulus; Arbitrary cross-section; Geometric characteristic; Fixed end force; Analytical methods

## 1. Introduction

Currently, most finite element analyses of existing structures are based on the principle of constant elastic modulus of materials. However, in reality, the elastic modulus of structural materials varies, exhibiting differences in tensile and compressive states, known as bimodulus. Numerous scholars have conducted research on bimodulus and achieved some results.

[1*] Prof., School of Intelligent Architecture, Changde College, Changde, China, School of Civil Engineering and Architecture, Hunan University of Arts and Science, Changde, China, e-mail: 352357749@qq.com

[2] Eng., School of Intelligent Architecture, Changde College, Changde, China, e-mail: 874638928@qq.com

Chang [1] investigated the large deflection deformation of thin shallow shells under uniformly distributed loads by considering bimodulus. Wu et al. [2] employed bimodulus elastic theory to calculate the flexural capacity of reinforced concrete members and compared the results with those obtained using relevant standard methods. Wu [3] and Wu et al. [4-7] determined the neutral layer positions of circular and rectangular cross-section beams based on bimodulus theory, derived formulas for the deflection, normal stress, shear stress of such beams, as well as the axial compressive buckling load formula for circular cross-section beams, demonstrating that transverse loads do not affect the neutral axis position of bimodulus beams. Li et al. [8] established a fatigue damage constitutive model considering bimodulus to analyze factors influencing surface damage in asphalt layers. Cheng et al. [9] analyzed the dynamic compressive-tensile modulus characteristics of asphalt mixtures, applied the compressive-tensile bimodulus to predict pavement responses, and explored the characteristics of pavement responses under a bimodulus system. Pan et al. [10] introduced bimodulus theory into pavement mechanical analysis, conducted numerical calculations for asphalt pavement structures considering bimodulus, and performed mechanical analyses on typical asphalt pavement structures.

Nayeban et al. [11] examined the behavior of beam composed of bimodulus materials using a granular micromechanics-based continuum model, and conduct comparative analysis of data with available experimental data. Misra and Placidi [12] exploited the granular micromechanics paradigm to present a simple continuum model within the isotropic framework in bimodulus system. Manickam et al. [13] conducted a research on the bending analysis of variable stiffness laminates of bimodulus composite materials subjected to mechanical and thermal loads. Valerii et al. [14] considered the variant of determining elastic moduli and Poisson’s ratios of bi-modulus materials based on the results of strain measurements by fiber Bragg grating sensors in rectangular specimens under four-point bending. Ribeiro and Silva [15] proposed a method to describe the bi-modular behavior of quasi-brittle materials. Václav et al. [16] proposed a novel method for studying the $\lambda/\mu$ ratio, the $v_P/v_S$ ratio and Poisson's ratio of rocks based on the determination of highly accurate moment tensors of acoustic emissions (AEs). Petrakov [17] conducted a research on the contact bending problem for a multilayer composite plate. Mauro and Ignacio [18] conduct a research which aims at contributing to a better understanding of the deformational behaviour of rocks, in particular when subjected to uniaxial tensile loads as well as in dealing with future updates of existing test methodologies. Ye et al. [19] put forward the theoretical and numerical approximation methods for the analysis of load-bearing characteristics of bimodulus sandwich structures. Hasan et al. [20] presented the numerical results and its analysis of transverse deflection and first mode free vibration of bimodular curved beam.

In summary, investigating the fixed end force analysis of prismatic member considering bimodulus is of significant theoretical importance. This research advances the engineering application of bimodular materials by deriving fixed-end force formulas and verifying their accuracy, highlighting that internal force and deflection analysis must account for the material's bimodular characteristics. Moreover, it serves as a fundamental basis for conducting finite element analysis of bimodulus bar structures.

## 2. Calculation of flexural rigidity with bimodulus

2.1 Theoretical analysis

Considering the bimodulus property, to determine the fixed-end forces of a prismatic member with a uniform cross-section, its flexural rigidity must first be calculated. To simplify the analysis, taking a rectangular section ($b \times h$) as an example, assuming the tensile modulus of elasticity is $E_t$ and the compressive modulus of elasticity is $E_c$, the flexural rigidity $D$ of section is shown in Fig. 1.

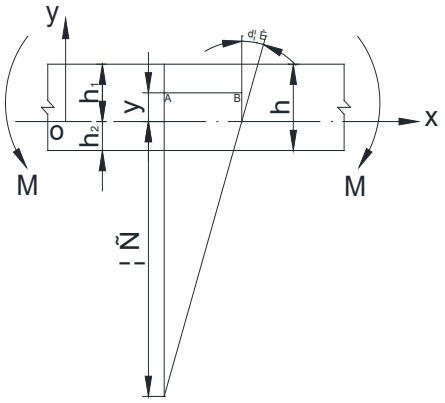


Fig. 1. Calculation diagram

Under pure bending conditions (subjected to moment $M$), according to the principle of plane section, the curvature of the neutral layer ($ox$ axis plane) satisfies $\frac{1}{\rho} = \frac{d\theta}{dx}$, and the relative elongation of the $AB$ layer at a distance of y from the neutral layer is $\varepsilon_x = \frac{y}{\rho} = y\frac{d\theta}{dx}$. From Fig. 1, it is not difficult to see that the longitudinal fibers above the neutral layer are under tension, while the longitudinal fibers below it are under compression. According to the generalized law of elasticity, the stress in these two parts is:

$$\sigma_x = \begin{cases} E_t \dfrac{y}{\rho}, & 0 < y \le h_1 \\ E_c \dfrac{y}{\rho}, & -h_2 \le y < 0 \end{cases} \tag{1}$$

Under the action of moment *M*, combined with the equilibrium equation of force $\int \sigma_x y dA = M$, we can obtain $\int_{-h_2}^{0} E_c \frac{y^2}{\rho} b dy + \int_{0}^{h_1} E_t \frac{y^2}{\rho} b dy = M$.

Combining $h_1 + h_2 = h$ and analyzing, it is concluded that $h_1 = \frac{h\sqrt{E_c}}{\sqrt{E_t} + \sqrt{E_c}}$, $h_2 = \frac{h\sqrt{E_t}}{\sqrt{E_t} + \sqrt{E_c}}$, flexural rigidity $D = \frac{b}{3}\left(E_t h_1^3 + E_c h_2^3\right)$. When the moment *M* is applied in the opposite direction, resulting in compression on the top and tension on the bottom, We can obtain $h_1 = \frac{h\sqrt{E_t}}{\sqrt{E_t} + \sqrt{E_c}}$, $h_2 = \frac{h\sqrt{E_c}}{\sqrt{E_t} + \sqrt{E_c}}$, flexural rigidity $D = \frac{b}{3}\left(E_c h_1^3 + E_t h_2^3\right)$.

The above analysis shows that for rectangular sections, the flexural rigidity *D* for the positive moment (compression on the top and tension on the bottom) region is equal to that of the negative moment ( tension on the top and compressionon the bottom) region. Generally, for asymmetric sections, the flexural rigidity *D* for the positive and negative moment regions is not equal. Therefore, when conducting force analysis, the flexural rigidity of the section should be considered in regions.

2.2 Programming design

An improved nodal line method combined with an iterative approach is adopted for the calculation of flexural rigidity with bimodulus. The principle for calculating the flexural rigidity of a bimodulus material is as follows: Firstly, input nodal line data and tensile and compressive elastic modulus to perform the calculation of sectional geometric properties, including area, moment of inertia, and position of the elastic neutral axis. Secondly, determine the position of the neutral axis at the nodal line. The calculation principle is shown in Fig. 2, and the determination formula is given in Equation (2). Finally, based on the determined position of the neutral axis, the flexural rigidity with bimodulus is calculated. The Program flowchart of calculation of flexural rigidity with bimodulus is shown in Fig. 3.

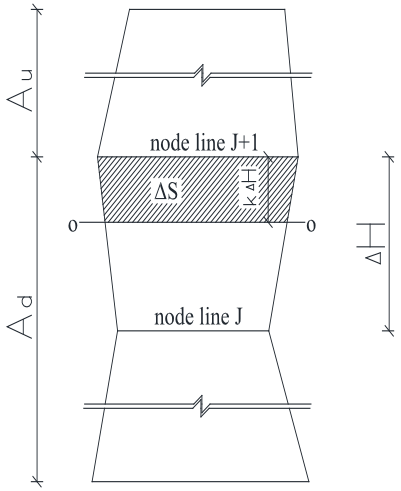


Fig. 2. Schematic diagram of judging the position of neutral axis at the node line for any cross-section

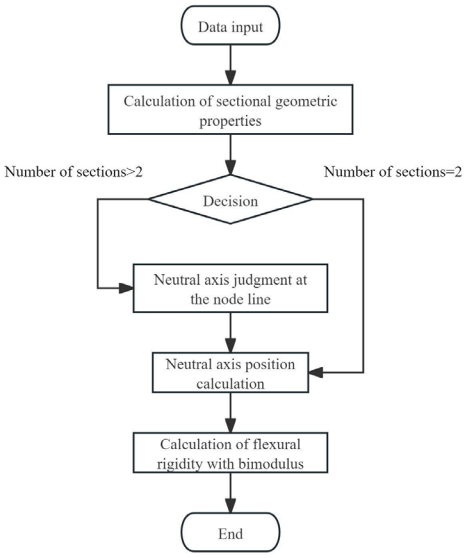


Fig. 3. Program flow chart

$$E_t\left(y_d A_d - A_d k\Delta H + \Delta S y_{\Delta S}\right) = E_c\left(y_u A_u + A_u k\Delta H + \Delta S y_{\Delta S}\right) \quad (2)$$

Where: $A_d$, $A_u$ are the areas of the lower and upper graphs relative to the joint line $J$+1 respectively; $y_d$, $y_u$ are the centroid distances of the lower and upper graphs to the joint line J+1 axis respectively; $k$ is the proportional coefficient, with a value range of 0 to 1.0, representing the ratio of the section height enclosed by the assumed neutral axis (OO axis) and the joint line $J$+1 (the shaded graph) to $\Delta H$; $\Delta S$ is the area of the shaded graph; $y_{\Delta S}$ is the distance of the centroid of shaded graph to the joint line $J$+1 axis. Formula (2) is solved using dichotomy iteration.

2.3 Program Verification

To verify the correctness of the program, assuming $E_t$= 3×10$^4$GPa, $E_c$=2.5×10$^4$GPa, rectangular section (25mm×100mm ) and T-shaped section (Web 180mm×1100mm, Flange 1500mm×200mm) have been selected for calculation. The specific calculation results and comparisons are shown in Tables 1 and Table 2.

*Table 1*

**Comparison Table of the Calculated Neutral Axis Heights for Bimodulus Materials (mm)**

| | Program value | | Theoretical value | | Error(%) | |
|---|---|---|---|---|---|---|
| | C/T | T/C | C/T | T/C | C/T | T/C |
| □ | 47.723 | 52.277 | 47.723 | 52.277 | 0 | 0 |
| T | 911.534 | 969.901 | 911.534 | 969.901 | 0 | 0 |

Note: “C/T” represents compression on the top and tension on the bottom, “T/C” represents tension on the top and compression on the bottom, the same applies below.

*Table 2*

**Comparison Table of the Calculated Flexural Rigidities for Bimodulus Materials (N.m$^2$)**

| | Program value | | Theoretical value | | Error(%) | |
|---|---|---|---|---|---|---|
| | C/T | T/C | C/T | T/C | C/T | T/C |
| □ | $5.6936\times10^4$ | $5.6936\times10^4$ | $5.6936\times10^4$ | $5.6936\times10^4$ | 0 | 0 |
| T | $2.0224\times10^9$ | $1.8791\times10^9$ | $2.0224\times10^9$ | $1.8791\times10^9$ | 0 | 0 |

Based on the data in Table 1 and Table 2, it is evident that the accuracy of the self-programmed calculation results meets the requirements.

## 3. Solution of fixed end force for propped cantilever beams

3.1 Subjected to a uniformly distributed load $q$

Assuming that, the length of Propped Cantilever beam is $L$, and it is subjected to a uniformly distributed load $q$. The flexural rigidity for positive moment (compression on the top and tension on the bottom) section is $D_1$, and for negative moment (tension on the top and compression on the bottom) section is $D_2$. The distance from zero moment position to the end of beam is $l_0$. The calculation model is shown in Fig. 4. Select a simply supported beam as the basic system (Fig. 5, where $f(x)$ is the external load and $f(x)$ is the uniformly distributed load $q$ here), and the redundant force is the end moment $x_1$.

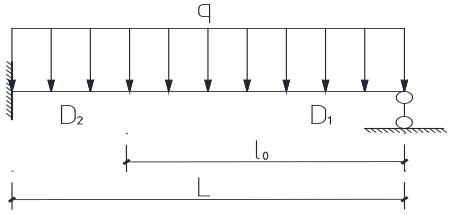


Fig. 4. Calculation Model

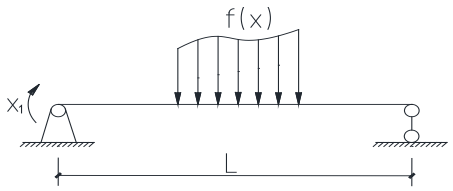


Fig. 5. Basic System

Formulate the force method equation from the displacement compatibility condition in the $x_1$ direction, as shown in Equation (3).

$$\delta_{11}x_1 + \Delta_{1p} = 0 \tag{3}$$

Where: $\delta_{11} = \int_0^{l_0} \frac{1}{D_1}\frac{x^2}{L^2}dx + \int_{l_0}^{l} \frac{1}{D_2}\frac{x^2}{L^2}dx$ ,

$\Delta_{1p} = \int_0^{l_0} \frac{1}{D_1}\frac{x}{L}\left(\frac{qLx}{2} - \frac{qx^2}{2}\right)dx + \int_{l_0}^{l} \frac{1}{D_2}\frac{x}{L}\left(\frac{qLx}{2} - \frac{qx^2}{2}\right)dx$ .

It can be solved to obtain $x_1 = -\frac{qL\left(D_1L^4 - 4D_1Ll_0^3 + 3D_1l_0^4 + 4D_2Ll_0^3 - 3D_2l_0^4\right)}{8\left(D_1L^3 - D_1l_0^3 + D_2l_0^3\right)}$.

Without considering bimodulus, $D_1 = D_2 = EI$ , $x_1 = -\frac{qL^2}{8}$ , $l_0 = \frac{4L}{5}$ .

3.2 Subjected to a concentrated load $F$

The element model is the same as Fig. 5, subjected to a concentrated load

*F*, with the zero moment at a distance of $l_0$ from the beam end, The calculation model is shown in Fig. 6, and the basic system is shown in Fig. 5 (*f* (*x*) is the concentrated load *F*).

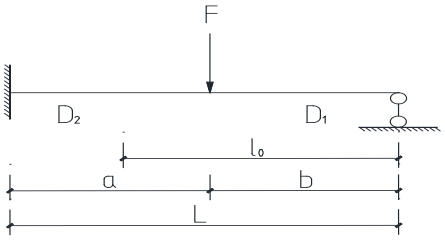


Fig. 6. Calculation Model

Similarly, the force method equation shown in equation (3) has been established, where the flexibility coefficient $\delta_{11}$ remains unchanged and the free term coefficient $\Delta_{1p}$ is shown in equation (4).

$$\Delta_{1p}=\int_0^b \frac{1}{D_1}\frac{x}{L}\frac{Fax}{L}dx+\int_b^{l_0}\frac{1}{D_1}\frac{x}{L}\left[\frac{Fax}{L}-F(x-b)\right]dx+\int_{l_0}^{l}\frac{1}{D_2}\frac{x}{L}\left[\frac{Fax}{L}-F(x-b)\right]dx \quad (4)$$

It can be solved to obtain $x_1=\dfrac{Fb\left[\left(D_1-D_2\right)\left(3l_0^2L-2l_0^3-L^3\right)+aD_2L\left(a-2L\right)\right]}{2\left(D_1L^3-D_1l_0^3+D_2l_0^3\right)}$.

Without considering bimodulus, $D_1=D_2=EI$, $x_1=-\dfrac{Fab\left(L+b\right)}{2L^2}$, $l_0=\dfrac{2L^3}{3L^2-b^2}$.

3.3 Subjected to a Concentrated moment *M*

The element model is the same as Fig. 5, subjected to a concentrated moment *M,* with the zero moment at distances of $l_a$, $l_b$=*b* from the beam end, respectively, The calculation model is shown in Fig. 7, and the basic system is shown in Fig. 5 (*f* (*x*) is the concentrated moment *M*).

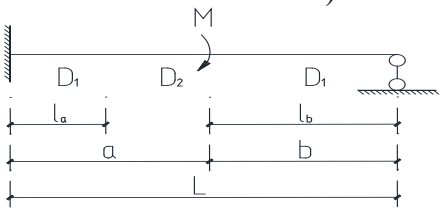


Fig.7. Calculation Model

Similarly, the force method equation shown in equation (3) has been established, where the flexibility coefficient $\delta_{11}$ and the free term coefficient $\Delta_{1p}$ are shown in equation (5).

$$\delta_{11}=\int_0^b \frac{1}{D_1}\frac{x^2}{L^2}dx+\int_b^{l-l_a}\frac{1}{D_2}\frac{x^2}{L^2}dx+\int_{l-l_a}^{l}\frac{1}{D_1}\frac{x^2}{L^2}dx$$

$$\Delta_{1p}=\int_0^b \frac{1}{D_1}\frac{x}{L}\frac{Mx}{L}dx+\int_b^{l-l_a}\frac{1}{D_2}\frac{x}{L}\left(\frac{Mx}{L}-M\right)dx+\int_{l-l_a}^{l}\frac{1}{D_1}\frac{x}{L}\left(\frac{Mx}{L}-M\right)dx \quad (5)$$

It can be solved to obtain

$$x_1 = -\frac{2M\{D_1\left[l_a^3 - \frac{3}{2}Ll_a^2 + \left(b + \frac{L}{2}\right)a^2\right] - D_2(b^3 - \frac{3}{2}Ll_a^2 + l_a^3)\}}{-2L^3D_1 + 2(D_1 - D_2)(b^3 + 3L^2l_a - 3Ll_a^2 + l_a^3)}.$$

Without considering bimodulus, $D_1 = D_2 = EI$ , $x_1 = \frac{M(L^2 - 3b^2)}{2L^2}$ , $l_a = \frac{(L^2 - 3b^2)L}{3(L^2 - b^2)}$ (When $l_a < 0$ , $l_a = 0$), $l_b = b$ .

## 4. Solution of fixed end force for two end fixed support beams

4.1 Subjected to a Uniformly distributed load *q*

Assuming that the length of two end fixed support beam is *L,* and it is subjected to a uniformly distributed load *q*, the flexural rigidity for positive moment section is $D_1$, and the flexural rigidity for negative moment section is $D_2$. The distance from zero moment position to the end of beam is $l_0$. The calculation model is shown in Fig. 8. Select a simply supported beam as the basic system (Fig. 9, where $f(x)$ is the external load and $f(x)$ is the uniformly distributed load $q$ here), and the redundant forces are the end moments $x_1$ and $x_2$, and the axial force $x_3$ at the member end.

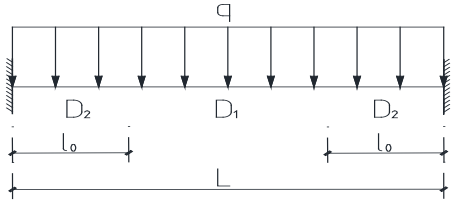


Fig.8. Calculation Model

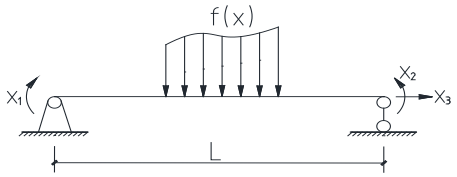


Fig. 9. Basic System

According to Fig. 9, it can be seen that $x_3$ has no effect on the moment of the beam and is not considered at this time. Only solutions $x_1$ and $x_2$ are required. Based on the displacement conditions in the $x_1$ and $x_2$ directions, establish the force method equations, as shown in equation (6).

$$\begin{cases} \delta_{11}x_1 + \delta_{12}x_2 + \Delta_{1p} = 0 \\ \delta_{21}x_1 + \delta_{22}x_2 + \Delta_{2p} = 0 \end{cases} \tag{6}$$

Where: $\delta_{11} = \int_0^{l_0} \frac{1}{D_2}\frac{x^2}{L^2}dx + \int_{l_0}^{l-l_0} \frac{1}{D_1}\frac{x^2}{L^2}dx + \int_{l-l_0}^{l} \frac{1}{D_2}\frac{x^2}{L^2}dx$ ,

$\delta_{12} = \delta_{21} = 2\int_0^{l_0} \frac{1}{D_2}\frac{x}{L}\left(1 - \frac{x}{L}\right)dx + \int_{l_0}^{l-l_0} \frac{1}{D_1}\frac{x}{L}\left(1 - \frac{x}{L}\right)dx$ , $\delta_{22} = \delta_{11}$ ,

$\Delta_{2p} = \Delta_{1p} = \int_0^{l_0} \frac{1}{D_2}\frac{x}{L}\left(\frac{qLx}{2} - \frac{qx^2}{2}\right)dx + \int_{l_0}^{l-l_0} \frac{1}{D_1}\frac{x}{L}\left(\frac{qLx}{2} - \frac{qx^2}{2}\right)dx + \int_{l-l_0}^{l} \frac{1}{D_2}\frac{x}{L}\left(\frac{qLx}{2} - \frac{qx^2}{2}\right)dx$ .

It can be solved to obtain $x_1 = x_2 = -\dfrac{q\left(6D_1Ll_0^2 - 4D_1l_0^3 + D_2L^3 - 6D_2Ll_0^2 + 4D_2l_0^3\right)}{12(2l_0D_1 + D_2L - 2D_2l_0)}$.

Without considering bimodulus, $D_1 = D_2 = EI$, $x_1 = x_2 = -\dfrac{qL^2}{12}$, $l_0 = \left(\dfrac{1}{2} - \dfrac{\sqrt{3}}{6}\right)L$.

4.2 Subjected to a concentrated load $F$

The element model is the same as Fig. 9, subjected to a concentrated load $F$, with the zero moment at a distance of $l_a$, $l_b$ from the beam end, The calculation model is shown in Fig. 10, and the basic system is shown in Fig. 9 ($f(x)$ is the concentrated load $F$).

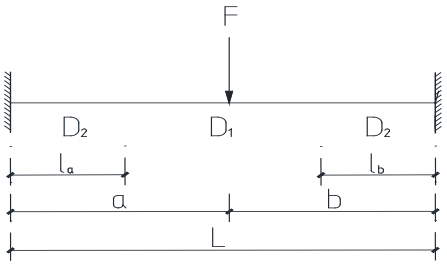


Fig. 10. Calculation Model

Establish the force method equations shown in equation (6), where the flexibility coefficient and free term coefficient are shown in equation (7).

$$\delta_{11} = \int_0^{l_b} \frac{1}{D_2}\frac{x^2}{L^2}dx + \int_{l_b}^{l-l_a} \frac{1}{D_1}\frac{x^2}{L^2}dx + \int_{l-l_a}^{l} \frac{1}{D_2}\frac{x^2}{L^2}dx$$

$$\delta_{12} = \delta_{21} = \int_0^{l_b} \frac{1}{D_2}\frac{x}{L}\left(1-\frac{x}{L}\right)dx + \int_{l_b}^{l-l_a} \frac{1}{D_1}\frac{x}{L}\left(1-\frac{x}{L}\right)dx + \int_{l-l_a}^{l} \frac{1}{D_2}\frac{x}{L}\left(1-\frac{x}{L}\right)dx$$

$$\delta_{22} = \int_0^{l_a} \frac{1}{D_2}\frac{x^2}{L^2}dx + \int_{l_a}^{l-l_b} \frac{1}{D_1}\frac{x^2}{L^2}dx + \int_{l-l_b}^{l} \frac{1}{D_2}\frac{x^2}{L^2}dx \tag{7}$$

$$\Delta_{1p} = \int_0^{l_b} \frac{1}{D_2}\frac{x}{L}\frac{Fax}{L}dx + \int_{l_b}^{b} \frac{1}{D_1}\frac{x}{L}\frac{Fax}{L}dx + \int_0^{l_a} \frac{1}{D_2}\left(1-\frac{x}{L}\right)\frac{Fbx}{L}dx + \int_{l_a}^{a} \frac{1}{D_1}\left(1-\frac{x}{L}\right)\frac{Fbx}{L}dx$$

$$\Delta_{2p} = \int_0^{l_a} \frac{1}{D_2}\frac{x}{L}\frac{Fbx}{L}dx + \int_{l_a}^{a} \frac{1}{D_1}\frac{x}{L}\frac{Fbx}{L}dx + \int_0^{l_b} \frac{1}{D_2}\left(1-\frac{x}{L}\right)\frac{Fax}{L}dx + \int_{l_b}^{b} \frac{1}{D_1}\left(1-\frac{x}{L}\right)\frac{Fax}{L}dx$$

It can be solved to obtain $x_1 = -\dfrac{AF}{B}$, $x_2 = \dfrac{CF}{H}$, we omit the expression of $A$,$B$,$C$,$H$ here due to space considerations. Without considering bimodulus, $D_1 = D_2 = EI$, $x_1 = -\dfrac{Fab^2}{L^2}$, $x_2 = -\dfrac{Fa^2b}{L^2}$, $l_a = \dfrac{aL}{L+2a}$, $l_b = \dfrac{bL}{L+2b}$.

4.3 Subjected to a Concentrated moment $M$

The element model is the same as Fig. 9, subjected to a concentrated moment $M$, the positions of the zero bending moment are at distances of $l_a$ and $l_b$ from the two ends of the beam, respectively. The calculation model is shown in Fig. 11, and the basic system is shown in Fig. 9 ($f(x)$ is the concentrated moment

*M*).

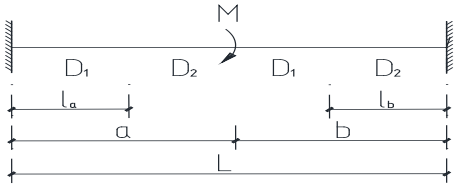


Fig. 11. Calculation Model

Establish the force method equations shown in equation (6), where the flexibility coefficient and free term coefficient are shown in equation (8).

$$
\begin{aligned}
\delta_{11} &= \int_0^{l_b} \frac{1}{D_2}\frac{x^2}{L^2}dx + \int_{l_b}^{b} \frac{1}{D_1}\frac{x^2}{L^2}dx + \int_0^{l_a} \frac{1}{D_1}(1-\frac{x}{L})^2 dx + \int_{l_a}^{a} \frac{1}{D_2}(1-\frac{x}{L})^2 dx \\
\delta_{12} = \delta_{21} &= \int_0^{l_b} \frac{1}{D_2}\frac{x}{L}\left(1-\frac{x}{L}\right)dx + \int_{l_b}^{b} \frac{1}{D_1}\frac{x}{L}\left(1-\frac{x}{L}\right)dx + \int_0^{l_a} \frac{1}{D_1}\frac{x}{L}\left(1-\frac{x}{L}\right)dx + \int_{l_a}^{a} \frac{1}{D_2}\frac{x}{L}\left(1-\frac{x}{L}\right)dx \\
\delta_{22} &= \int_0^{l_a} \frac{1}{D_1}\frac{x^2}{L^2}dx + \int_{l_a}^{a} \frac{1}{D_2}\frac{x^2}{L^2}dx + \int_0^{l_b} \frac{1}{D_2}(1-\frac{x}{L})^2 dx + \int_{l_b}^{b} \frac{1}{D_1}(1-\frac{x}{L})^2 dx \\
\Delta_{1p} &= \int_0^{l_b} \frac{1}{D_2}\frac{x}{L}\frac{Mx}{L}dx + \int_{l_b}^{b} \frac{1}{D_1}\frac{x}{L}\frac{Mx}{L}dx - \int_0^{l_a} \frac{1}{D_1}\left(1-\frac{x}{L}\right)\frac{Mx}{L}dx - \int_{l_a}^{a} \frac{1}{D_2}\left(1-\frac{x}{L}\right)\frac{Mx}{L}dx \\
\Delta_{2p} &= -\int_0^{l_a} \frac{1}{D_1}\frac{x}{L}\frac{Mx}{L}dx - \int_{l_a}^{a} \frac{1}{D_2}\frac{x}{L}\frac{Mx}{L}dx + \int_0^{l_b} \frac{1}{D_2}\left(1-\frac{x}{L}\right)\frac{Mx}{L}dx + \int_{l_b}^{b} \frac{1}{D_1}\left(1-\frac{x}{L}\right)\frac{Mx}{L}dx
\end{aligned}
\tag{8}
$$

It can be solved to obtain $x_1 = \frac{AM}{B}$, $x_2 = \frac{CM}{H}$, we omit the expression of *A*,*B*,*C*,*H* here due to space considerations. Without considering bimodulus, $D_1 = D_2 = EI$, $x_1 = \frac{Mb(3a-L)}{L^2}$, $x_2 = -\frac{Ma(3b-L)}{L^2}$, $l_a = \frac{L}{2} - \frac{L^2}{6a}$, $l_b = \frac{L}{2} - \frac{L^2}{6b}$.

## 5. Analysis and Verification

In order to verify the correctness of the derivation of the fixed end force mentioned above, assuming $E_t$= 3×10$^4$ GPa and $E_c$=2.5×10$^4$ GPa. Used ANSYS finite element software, selected SOLID185 elements, the force analysis of rectangular section beams and T-shaped section beams with propped cantilever support and both ends fixed support have been conducted.

5.1 Propped Cantilever beams analysis

5.1.1 rectangular section beam analysis

The length of a propped cantilever beam with rectangular section (25mm×50mm) is 1 m. The concentrated load *F* at the mid span is 10 kN or the uniformly distributed load *q* is 10 kN/m, and the flexural rigidity *D* for bimodulus is 7.1170×10$^9$ N.mm$^2$. The comparison between the ANSYS calculation results and the calculation results using the formula in this article is shown in Table 3.

*Table 3*

**Comparison of calculation results for rectangular section beams with propped cantilever supports**

| | fixed-end moment(N.m) | | | Fixed end shear force (N) | | |
|---|---|---|---|---|---|---|
| | ANSYS value | Theoretical value | Error(%) | ANSYS value | Theoretical value | Error(%) |
| F | 1875 | 1875 | 0 | 1875 | 6875 | 0 |
| q | 1250 | 1250 | 0 | 6250 | 6250 | 0 |

Note: The error in the table is calculated as (theoretical value - ANSYS value)/ANSYS value×100%, the same applies below. ANSYS calculations show that: Subjected to the Concentrated force $F$, $l_0$=727.5 mm, Subjected to the uniformly distributed load $q$, $l_0$= 750.0 mm。

It is not difficult to see from Table 3 that the ANSYS calculation results are consistent with the calculation results using the formula in this article, indicating that the formula in this article is accurate and effective.

ANSYS software analysis shows that: under the action of load, the internal force distribution along the axis direction of the beam is consistent with that without considering bimodulus for rectangular section with bimodulus. The analysis of equations (6) and (8) also verifies this viewpoint. But, there is a significant difference in deflection, and the reason for this is that the elastic stiffness of the section ( $EI = E\frac{bh^3}{12}$ ) is not equal to the flexural rigidity of the section ( $D = \frac{b}{3}\left(E_t h_1^3 + E_c h_2^3\right)$ ).

5.1.2 T-shaped section beam analysis

The length of a Propped Cantilever beam with T-shaped section (50mm×40mm×15mm×15mm) is 1m. The concentrated load $F$ at the mid span is 10 kN or the uniformly distributed load $q$ is 10 kN/m, and the flexural rigidity for bimodulus is $D_1$=6.6871×10$^9$ N.mm$^2$ and $D_2$=6.4220×10$^9$ N.mm$^2$. The comparison between the ANSYS calculation results and the calculation results using the formula in this article is shown in Table 4.

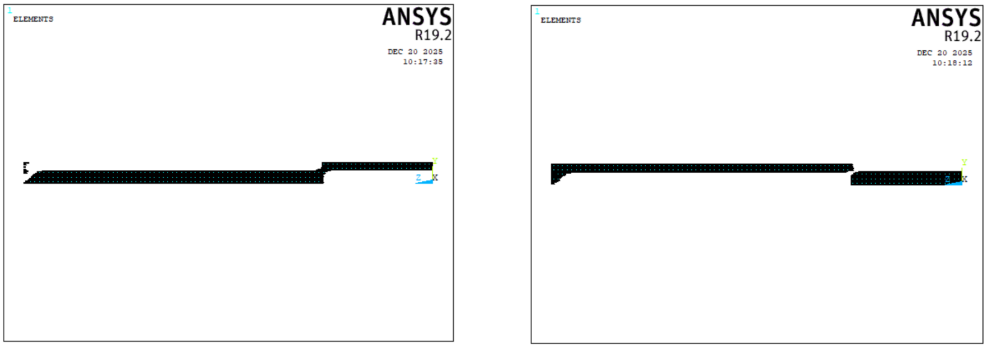


(a) tensile zone of the beam (b) compressive zone of the beam

Fig.12 Diagram of the tensile and compressive regions of the beam (*F*)

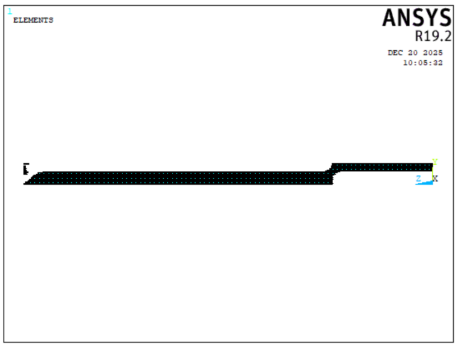


(a) tensile zone of the beam

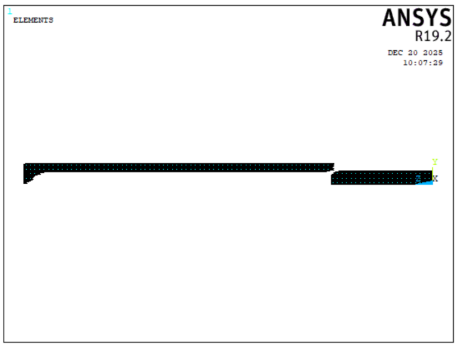


(b) compressive zone of the beam

Fig.13 Diagram of the tensile and compressive regions of the beam (*q)*

*Table 4*

**Comparison of calculation results for T-shaped beams with propped cantilever supports**

| | fixed-end moment(N.m) | | | Fixed end shear force (N) | | |
|---|---|---|---|---|---|---|
| | ANSYS value | Theoretical value | Error(%) | ANSYS value | Theoretical value | Error(%) |
| F | 1847.039 | 1846.925 | -0.006 | 6847.039 | 6846.925 | -0.002 |
| q | 1234.214 | 1234.054 | -0.013 | 6234.214 | 6234.054 | -0.003 |

Note: ANSYS calculations show that: Subjected to the Concentrated force $F$, $l_0$=730.2 mm, Subjected to the uniformly distributed load $q$, $l_0$=753.2 mm.

It is not difficult to see from Fig. 12 and Fig. 13 that there is a certain range for reversal of bending moment, that is, the zero moment section spans a certain region, it is not an abrupt point. Considering the Saint Venant principle, there is a local tension region at the top of the simply supported position, and about the height of the beam near the simply supported position, the tension and compression region of the beam are complex, and it is not conform to the basic principles of material mechanics. It is easy to see from Table 4 that the ANSYS calculation results are very close to the calculation results using the formula in this article, with very small errors.

Under the concentrated load $F$ at the mid span, without considering bimodulus, the fixed end moment is 1.875 kN.m, the fixed end shear force is 6875 N, and the mid span deflection is 13.279 mm. Considering bimodulus, the fixed end moment is 1.847 kN.m, the fixed end shear force is 6847 N, and the mid span deflection is 14.483 mm. In contrast, without considering bimodulus, The errors in the fixed end moment, the fixed end shear force and the mid span deflection are 1.52%, 0.41% and 8.31%, respectively. Continuing analysis shows that when $E_t : E_c \notin (0.667, 1.5)$, the error in fixed end moment and fixed end shear force without considering bimodulus exceeds 5.0%, and the deflection error at the mid span exceeds 30.1%.

Under the uniformly distributed load $q$, without considering bimodulus, the fixed end moment is 1.250 kN.m, the fixed end shear force is 6250 N, and the mid span deflection is 7.702 mm. Considering bimodulus, the fixed end moment

is 1.234 kN.m, the fixed end shear force is 6234 N, and the mid span deflection is 8.401 mm. In contrast, without considering bimodulus, The errors in the fixed end moment, the fixed end shear force and the mid span deflection are 1.30%, 0.26% and 8.32%, respectively. Continuing analysis shows that when $E_t : E_c \notin (0.667, 1.5)$, the error in fixed end moment and fixed end shear force without considering bimodulus exceeds 5.0%, and the deflection error at the mid span exceeds 29.9%.

5.2 Two end fixed T-shaped section beam analysis

The length of two end fixed T-shaped section (50mm×40mm×15mm×15mm) beam is 1m, the concentrated load $F$ is 10 kN at the mid span or the uniformly distributed load $q$ is 10 kN/m, the flexural rigidity of bimodulus are $D_1$=6.6871×10$^9$ N.mm$^2$ and $D_2$=6.4220×10$^9$ N.mm$^2$. The tensile and compressive regions of the beam are shown in Fig. 14 and Fig. 15 by ANSYS software. The comparison of calculation results is shown in Table 5.

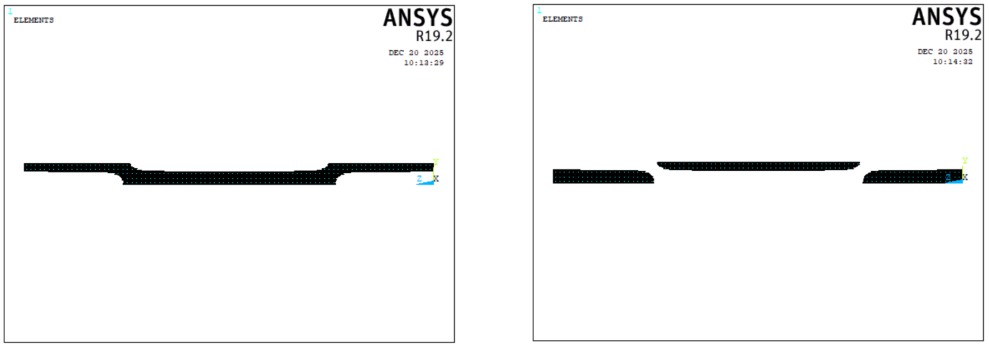


(a) tensile zone of the beam (b) compressive zone of the beam

Fig.14 Diagram of the tensile and compressive regions of the beam (*F*)

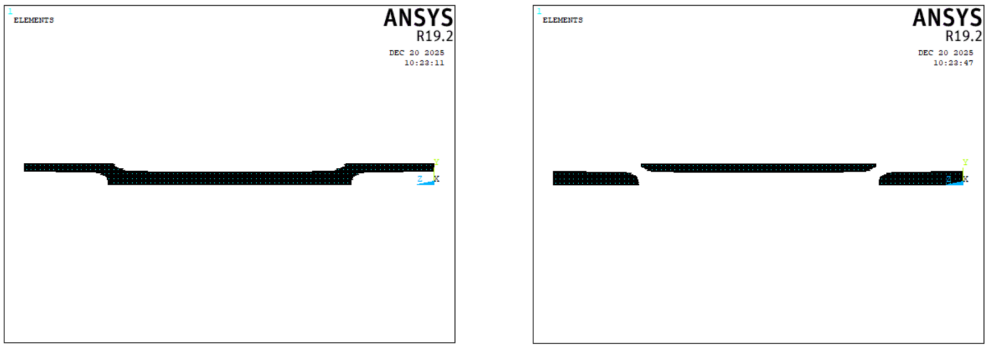


(a) tensile zone of the beam (b) compressive zone of the beam

Fig.15 Diagram of the tensile and compressive regions of the beam (*q*)

*Table 5*

**Comparison of calculation results for T-shaped beams with fixed supports at both ends**

| | fixed-end moment(N.m) | | | Fixed end shear force (N) | | |
|---|---|---|---|---|---|---|
| | ANSYS value | Theoretical value | Error(%) | ANSYS value | Theoretical value | Error(%) |
| F | 1237.366 | 1237.360 | -0.0005 | 5000 | 5000 | 0 |
| q | 826.585 | 826.826 | 0.0292 | 5000 | 5000 | 0 |

Note: ANSYS calculations show that: Subjected to the Concentrated force $F$ at the mid span, $l_a = l_b$ =247.5 mm, Subjected to the uniformly distributed load $q$, $l_0$=209.0 mm.

As can be easily seen from Fig. 14 and 15 that there is a certain range of changes from positive moment to negative moment or reverse, that is, the zero moment section spans a certain region, it is not a sudden change and does not conform to the basic principles of material mechanics. It is not difficult to see from Table 5 that the ANSYS calculation results are very close to the calculation results using the formula in this article, with very small errors.

Under the concentrated load $F$ at the mid span, Without considering bimodulus, the fixed end moment is 1.25 kN.m, the fixed end shear force is 5000 N, and the mid span deflection is 7.577 mm. Considering bimodulus, the fixed end moment is 1.237 kN.m, the fixed end shear force is 5000 N, and the mid span deflection is 8.282 mm. In contrast, without considering bimodulus, The errors in the fixed end moment, the fixed end shear force and the mid span deflection are 1.05%, 0 and 8.51%, respectively. Continuing analysis shows that when $E_t : E_c \notin (0.443, 2.257)$ the error in fixed end moment and fixed end shear force without considering bimodulus exceeds 5.0%, and the deflection error at the mid span exceeds 30.22%.

Under uniformly distributed load $q$, without considering bimodulus, the fixed end moment is 0.833 kN.m, the fixed end shear force is 5000 N, and the mid span deflection is 3.755 mm. Considering bimodulus, the fixed end moment is 0.827 kN.m, the fixed end shear force is 5000 N, and the mid span deflection is 4.113 mm. In contrast, without considering bimodulus, The errors in the fixed end moment, the fixed end shear force and the mid span deflection are 0.73%, 0 and 8.71%, respectively. Continuing analysis shows that when $E_t : E_c \notin (0.417, 2.395)$ the error in fixed end moment without considering bimodulus exceeds 5.0%, the deflection error at the mid span exceeds 32.40%.

## 6. Conclusions

Except for symmetrical sections such as rectangles, the flexural rigidity $D$ for the positive moment region and that for the negative moment region of generally asymmetric sections are not equal. ANSYS solid element analysis verification shows that the derived formula is accurate and effective. The bending moment does not reverse at a single point but over a finite region, known as

the zero-moment zone. Under the bimodulus theory, although the internal force distribution along the beam axis for a loaded rectangular section is identical to that predicted by classical (single-modulus) theory, the resulting deflection is markedly different. When the load is applied to other asymmetric sections, the internal force distribution is inconsistent with that without considering bimodulus, and the difference in deflection is significant and the error is large. When the ratio of tensile and compressive elastic modulus of the material exceeds a certain range, the error in the fixed end force exceeds 5%, and the error in the deflection will exceed 30%, which is unacceptable.

At present, there is relatively little research on the force analysis of frame structures with bimodulus. Several formulas for fixed end forces under load are derived in this article, which are only applicable to the analysis of planar frame structures. For spatial frame structures, especially considering plates with bimodulus, further research is needed in the future.

**Acknowledgements**

This work was supported by the Hunan Provincial Natural Science Foundation Project (2021JJ50136).

## REFERENCES

[1] *Chang H*. Large-deflection deformation problems of thin shallow shell structures with different moduli in tension and compression. Chongqing University, 2023.

[2] *Wu X*, *Yang L J*, *Huang Z G*. Calculation for normal section bearing capacity of reinforced concrete members using the constitutive relation. Building Structure,2014, 44(9):68-71

[3] *Wu X*. Bending calculation of circular section beams with different elastic modulus of tension and compression. Journal of Natural Science of Hunan Normal University, 2022, 45(5):144-149

[4] *Wu X*, *Luo Y X*. Effects of shear deformation on bending normal stress of bimodulous beam. Journal of Hunan University of Arts and Science(Science and Technology), 2016, 28(1):55-59

[5] *Wu X*, *Yang L J*, *Huang Z G*. Calculating performance parameters of bimodulous material with shear effect principle. Journal of Central South University (Science and Technology),2014,45(2):609-614

[6] *Wu X*, *Liu Q Y*, *Luo Y X*. Calculating bending deflection of bimodulous deep beam by energy method. Chinese Quarterly Of Mechanics,2017,38(3): 586-591

[7] *Wu X*, *Xiao Z*. Elastic buckling of the double modulus beam with circular section under axial compression. Journal of Natural Science of Hunan Normal University, 2024,47(06):132-140.

[8] *Li S*, *Sun Y*, *Yu S Q*, *et al*. Top-down fatigue crack control and damage analysis of continuous reinforced cement concrete composite asphalt pavement base on bi-modulus theory. China Civil Engineering Journal, 2024, 57(04):111-128.

[9] *Cheng H, Sun L, Zheng J, et al.* Dynamic compressive-tensile moduli of asphalt mixture and its applications to pavement response prediction. China Civil Engineering Journal, 2022, 55(3): 105-116.

[10] *Pan X Q*, *Zheng J L*. Mechanical calculation method and analysis of asphalt pavement considering different modulus in tension and compression. China Civil Engineering Journal, 2020,53(11): 110-117.
[11] *Nayeban M M, Fabbrocino F, Placidi L, et al.* Analysis of beams composed of bimodulus materials treated by granular micromechanics. Available at SSRN 5269249.
[12] *Misra A, Placidi L.* Emergence of bimodulus (tension–compression asymmetric) behavior modeled in granular micromechanics framework. Mathematics and Mechanics of Solids, 2025: 10812865241299340.
[13] *Manickam G, Balaji L, Polit O, et al.* Bimodulus composite materials based variable stiffness laminates using curvilinear fibre-reinforced layers-static bending characteristics under mechanical and thermal loadings. Composite Structures, 2025, 365: 119183.
[14] *Valerii M, Grigorii S, Andrey F, et al.* Determination of elastic moduli and Poisson's ratios of bi-modulus materials based on the results of four-point bending test. Materials and Structures, 2024, 57(4): 96.
[15] *Ribeiro G C, Silva S P*. Formulation based on combined loading function strategy to improve the description of the bi-modularity of quasi-brittle material degradation with multiple damage evolution laws. Applied Mathematical Modelling, 2024, 126: 713-738.
[16] *Vavryčuk V, Petružálek M, Lokajíček T, et al.* Bi-modular properties of sandstone inferred from seismic moment tensors of acoustic emissions. International Journal of Rock Mechanics and Mining Sciences, 2023, 171: 105576.
[17] *Petrakov I E.* Contact Bending Problem for a Multilayer Composite Plate with Allowance for Different Moduli of Elasticity in Tension and Compression. Journal of Applied and Industrial Mathematics, 2022, 16(4): 751-759.
[18] *Mauro M, Ignacio P.* Intact rock deformation bimodularity: an experimental study. IOP Conference Series: Earth and Environmental Science. IOP Publishing, 2023, 1124(1): 012041.
[19] *Ye Z, Li X, Xu Z, et al.* Theoretical and Numerical Approximation Methods for Predicting Bending Characteristics of Bimodulus Sandwich Structures. Acta Mechanica Solida Sinica, 2023, 36(3): 443-456.
[20] *Hasan S N, Kumar A, Khan K.* Bending and undamped free vibration analysis of laminated bimodular composite Material thin curved beam. Materials Today: Proceedings, 2022, 61: 10-15.